Density Functional Theory (DFT) Studies of electronic structures and photoelectrical properties of Coumarin-based Dyes—Applications to Dye-Sensitized Solar Cells

Said H.Vuai and Numbury Surendra Babu,
Department of Chemistry, College of Natural and Mathematical sciences
The University of Dodoma, Post Box: 338, DDODOMA, TANZANIA.

Abstract
To get compelling sensitizer, a progression of D-π-A metal free dyes has been planned by altering the giving and acceptor gathering. In the present research article to approach to manage improving the execution of coumarin dye photosensitizers are the differences in different acceptor gatherings and depicted hypothetically. The photoelectrical properties of Coumarin based Dyes as sensitizers of dye-sensitized solar cells were investigated through density functional theory (DFT) and time-dependent (TD-DFT). The key parameters including the light harvesting efficiency (LHE), the driving force of electron injection (ΔG_{inject}) and dye regeneration (ΔG_{regen}), the total dipole moment (μnormal), and the excited state lifetime(τ)were investigated, which are closely related to the short-circuit current density(Jsc) and open circuit voltage(Voc).We give the electronic structure and simulated UV-Vis spectra of the dyes and the HOMO and LUMO orbital electron densites and investigate the electron exchange from the dye to the semiconductor titanium dioxide (TiO_2). Likewise, these novel sensitizers would be a promising contender for upgrading the execution of the DSSCs.

Keywords: Coumarin dye dyes, DFT/TDDFT, Absorption spectra, HOMO and LUMO energies, optoelectronic properties

1. Introduction

Dye-sensitized solar cells (DSSC) have pulled in impressive enthusiasm in the course of the most recent couple of years, as they offer the benefits of low manufacture costs, straightforwardness and adaptability, when wanted [1]. For such reasons, DSSCs may give a decision to moderate low power age in urban/ rural regions and, specifically, a plausibility of delivering power creating windows [2, 3]. Since 1991, Grätzel et al. [4] presented the nanocrystalline permeable electrode with an extraordinary proportion surface territory and a organic electrolyte to Dye-sensitized solar cells (DSSC). A few specialists have examined their utilization in creating nanostructured films [5-7] enhancing photovoltaic devices [8-10] and a general logical comprehension of charge-exchange between material interfaces [11-12].

In DSSCs three types of sensitizers are utilized: (I) ruthenium (Ru) based dye sensitizers, (ii) porphyrin and (iii) metal free organic sensitizers design of donor-π-acceptors (D-π-A). Ruthenium polypyridyl complex photosensitizers (e.g N3dye) designed by Gra¨tzel and associates, have been effectively intended for productive DSSCs. They give wide absorption spectra reaching out into the close IR region by introduction of thiocyanato ligands (- NCS) and demonstrated a strong electron donor ability. The N3 dye produce solar energy-to-electricity conversion efficiencies (η) of up to 11% under AM 1.5G illumination w with a nanocrystalline TiO_2 electrode and the iodine redox electrolyte [13-20].

It is far-fetched that the supply as well as cost of ruthenium will permit such DSSCs to be generally received as required for a genuine solar based economy. Up to this point, the general power transformation proficiency (PCE, η) of Ru complexes and zinc porphyrin sensitizers have achieved 13% [21]. Anyway the porphyrin dyes synthesis is exorbitant and troublesome on the grounds that it include a "push-pull" structure with substituent "push" and "pull"groups. Contrasted and the other two kinds of dyes, organic D-π-A dyes have gotten a regularly expanding consideration because of their lower cost, simple of manufacture, relative higher molar extinction coefficients and ecological inviting.

Organic dyes have a few favorable circumstances as photosensitizers: (a) they are less expensive than Ru edifices, (b) they have extensive absorption coefficients because of intramolecular π-π* transitions, and (c) there are no worries about constrained assets, since they don't contain respectable metals, for example, ruthenium. To the extent the sensitizers are concerned, various investigations have demonstrated that every single organic sensitizer with a D-π-A, D-π-D-π-A, or D-π-A-π-A structure, where D and A are electron donating and withdrawing groups, respectively, offer a few favorable circumstances over organometallic compounds, for example, higher molar extinction coefficients, easier synthesis, and reduced production cost.

Coumarin-based dyes have been effectively utilized in dye-sensitized solar cells (DSSC), prompting photovoltaic conversion efficiencies of up to around 8%. Coumarin-based dyes ones have demonstrated great photoresponse in the visible region, long haul dependability under exposure and appropriate energy level arrangement for injection into the conduction band of TiO_2. Coumarin remain as an exceptionally intriguing class of compounds , given the quick injection rates observed to TiO_2 substrates,[22] and the

accessibility of a vast scope of synthetic derivatives that display especially unique properties[23– 26]. Actually, by carefully choosing their molecular structure, the execution of coumarin-based DSSC has been fundamentally improved, by diminishing accumulation issues and enhancing both absorption and redox properties.

As of late, quantum chemical methods have turned into a doable intends to uncover the connection among structures and properties of dye molecules, which give a dependable theoretical premise to the fast screening of very proficient dye molecules [27]. Numerous analysts have prevailing with regards to foreseeing the photoelectric properties of dyes and organic molecules in light of the quantum synthetic strategies [28].

A few computational investigations of coumarin based dyes have been published, explaining some of the exceptionally good characteristic of these dyes. One of the principal such examination was accounted for by Hara et al., [29] and was centered on the calculation of the oxidation and reduction potentials of various early coumarin based dyes. Performing DFT and TD-DFT estimations, Kurashige et al. [30] explored the energized conditions of the coumarin colors, Preat and collaborators [31] examined the electronic spectra, while Zhang et al.,[32]. Zhang and teammates displayed a systematical examination on the key parameters including the open circuit voltage and short out current density of dyes in view of density functional theory (DFT) and time-dependent DFT (TD-DFT) calculations, and proposed basic changes, which would enhance the light absorption and energy level arrangement. All the more as of late, Sanchez-de-Armas et al. [33] tended to a few necessities for the DSSC sensitizers, for example, the position and width of the principal band in the electronic absorption spectra, the absorption threshold and the LUMO energy concerning the conduction band edge of the semiconductor.

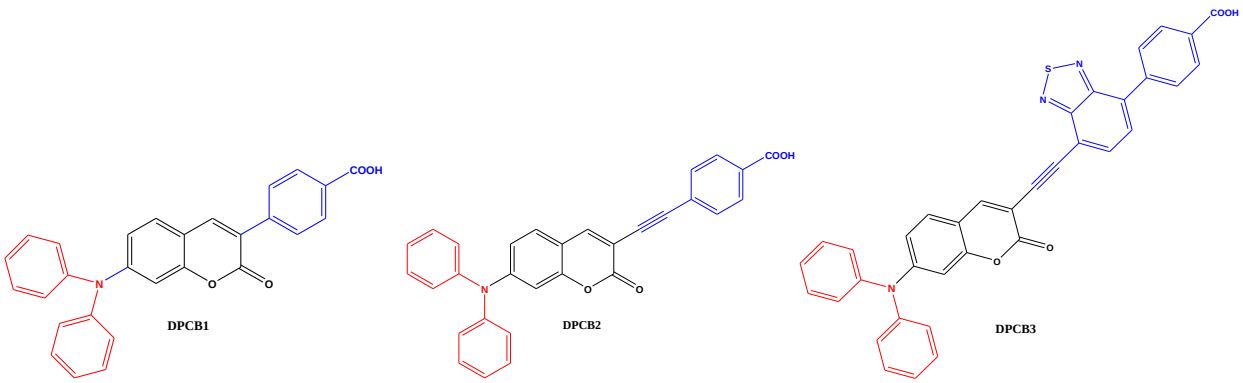

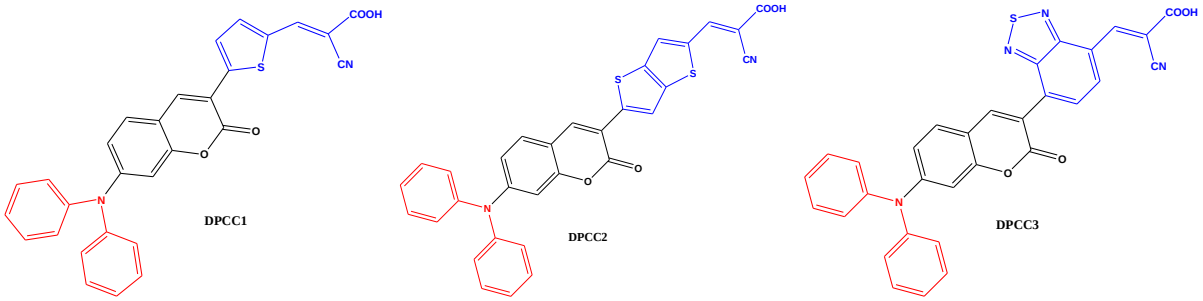

Scheme 1: Molecular structures of coumarin-based dyes. Red color group is donor (D) and blue color is acceptor (A).

In this paper, we present a definite examination of six new diphenylamine coumarin based dyes with various acceptor groups. The molecular structures of coumarin-based dyes are appeared in Scheme 1. The computational studies have been led with the six sensitizers in gas and acetonitrile solvent. The key parameters which are firmly identified with the short out current density(Jsc) and open circuit voltage (Voc), including the light harvesting efficiency (LHE), the driving force of electron injection (ΔG_{inject}) , dye regeneration (ΔG_{regen}), the total dipole moment (μnormal), and in addition, the excited state lifetime (τ).The expounded calculations will give a premise to clarifying the hypothetically unique photoelectrical properties between the six colors and build up the potential utility in DSSCs.

In this paper, we tend to gift a certain examination of six new diphenylamine coumarin based mostly dyes with numerous acceptor teams. The molecular structures of coumarin-based dyes are appeared in theme one. The computational studies are carried out with the six sensitizers in gas phase and acetonitrile solvent. The key parameters that are firmly known with the short current density (J_{sc}) and open circuit photo voltage (Voc), together with the light harvesting efficiency (LHE), the injection driving force (ΔGinject) , dye regeneration energy(ΔGregen), the dipole moment (μnormal), and additionally, the life time of the electrons (τ).The expounded calculations can provides a premise to instructive the hypothetically distinctive electricity properties between the six dyes and build up the potential utility in DSSCs.

2. Computational Details

2.1 Theoretical Background. The power conversion efficiency (η) of the DSSCs can be determined by the J_{sc}, V_{oc}, and the fill factor (ff) and it can be calculated according to the following equation [34]

$$\eta = \frac{FFV_{oc}J_{sc}}{P_{inc}} \quad (1)$$

where P_{inc} is the incident power density, J_{sc} is the short-circuit current, V_{oc} is the open-circuit voltage, and FF denotes the fill factor.

The J_{SC} in DSSCs is determined by the following equation [35]

$$J_{sc} = \int LHE(\lambda)\Phi_{inject}\eta_{collect}d\lambda \quad (2)$$

The J_{sc} factor for a given dye and cell design can be determined by integrating the incident to current efficiency (IPCE) on the energetic space [36]

$$J_{sc} = \int_{\lambda} IPCE(\lambda)d\lambda \quad (3)$$

Where the IPCE is given by

$$IPCE(\lambda) = LHE(\lambda)\Phi_{\text{inject}}\eta_{\text{collect}} \quad (4)$$

where LHE(λ) is the light harvesting efficiency at a given wavelength, Φ_{inject} evinces the electron injection efficiency, and $\eta_{collect}$ denotes the charge collection efficiency. In the systems which are only different in sensitizers, $\eta_{collect}$ can be reasonably assumed to be constant. LHE (λ) can be calculated from the following equation

$$LHE = 1 - 10^{-f} \quad (5)$$

where f represents the oscillator strength of adsorbed dye molecules. Φ_{inject} is related to the driving force ΔG_{inject} of electrons injecting from the excited states of dye molecules to the semiconductor substrate. It can be estimated as [37]

$$\Delta G_{inject} = E_{OX}^{dye*} - E_{CB}^{TiO_2} = E_{OX}^{dye} + E_{0-0}^{dye} - E_{CB}^{TiO_2} \quad (6)$$

From the equations 5−9, we could roughly predict the efficiency of novel dyes without intensive calculations.

Where E_{OX}^{dye*} is the oxidation potential of the excited dye, E_{OX}^{dye} is the redox potential of the ground state of the dye, E_{0-0}^{dye} is the vertical transition energy, and $E_{CB}^{TiO_2}$ is the conduction band edge of the TiO_2

semiconductor. So J_{SC} can be well estimated through f and ΔG_{inject}. Two models can be used for the evaluation of E_{OX}^{dye*} [38]. The first implies that the electron injection occurs from the un relaxed excited state. For this reaction path, the excited state oxidation potential can be extracted from the redox potential of the ground state, E_{OX}^{dye} which has been calculated at the B3LYP-6-31G(d) approach and the vertical transition energy corresponding to the photoinduced intermolecular CT (ICT),

$$E_{OX}^{dye*} = E_{OX}^{dye} - \lambda_{\max}^{ICT} \quad (7)$$

where $\lambda_{\max}^{ICT}$ is the energy of the ICT. Note that this relation is only valid if the entropy change during the light absorption process can be neglected. For the second model, one assumes that electron injection occurs after relaxation. Given this condition, E_{OX}^{dye} is expressed as [39]:

$$E_{OX}^{dye*} = E_{OX}^{dye} - E_{0-0}^{dye} \quad (8)$$

As for Voc in DSSCs, it can be described by:[40]

$$V_{oc} = \frac{E_{CB} + \Delta E_{CB}}{q} + \frac{k_b T}{q} \ln\left(\frac{n_c}{N_{CB}}\right) - \frac{E_{redox}}{q} \quad (9)$$

Where q is the unit charge, E_{CB} is the conduction band edge of the semiconductor substrate, k_bT is the thermal energy, n_c is the number of electrons in the conduction band, N_{CB} is the density of accessible states in the conduction band, and E_{redox} is the electrolyte Fermi level. $\triangle E_{CB}$ is the shift of E_{CB} when the dyes are adsorbed on substrate and can be expressed as:[41]

$$\Delta E_{CB} = -\frac{q\mu_{normal}\gamma}{\varepsilon_0 \varepsilon} \quad (10)$$

Here, μ_{normal} is the dipole moment of individual dye perpendicular to the surface of semiconductor substrate. γ is the surface concentration of dyes. ε_0 and ε represent the vacuum permittivity and the dielectric permittivity, respectively. It is clear that μ_{normal} would exert crucial influence on V_{OC}.

To analyze the relationship between V_{OC} and E_{LUMO} of the dyes based on electron injection (in DSSCs) from LUMO to the conduction band of semiconductor TiO_2 (E_{CB}), the energy relationship can be expressed [42]:

$$V_{oc} = E_{LUMO} - E_{CB} \quad (11)$$

The obtained values V_{oc} of the studied dyes calculated according to the Eq. 2 range from 1.0535 eV to 1.4955 eV of TiO_2 (Tab. 3) these values are sufficient for a possible efficient electron injection.

2.1.1 Electron injection. The description of the electron transfer from a dye to a semiconductor, the rate of the charge transfer process can be derived from the general classical Marcus theory, [43-45].

$$k_{inject} = |V_{RP}|(2/h(\pi/\lambda k_B T)1/2\exp[-(\Delta G^{inject} + \lambda)2/4\lambda k_B T] \quad (12)$$

In eq. (12), k_{inject} is the rate constant (in s^{-1}) of the electron injection from dye to TiO_2, k_B is the Boltzmann thermal energy, h the Planck constant, G^{inject} is the free energy of injection, $|V_{RP}|$ is the coupling constant between the reagent and the product potential curves. Eq (11) revealed that larger $|V_{RP}|$ leads to higher rate constant which would result better sensitizer. The use of the Generalized Mulliken-Hush formalism (GMH) allows evaluating |VRP| for a photoinduced charge transfer [41, 42]. Hsu et al. explained that |VRP| can be evaluated as [44]

$$|V_{RP}| = \frac{\Delta E_{RP}}{2} \quad (13)$$

The injection driving force can be formally expressed within Koopmans approximation as

$$\Delta E_{RP} = \left[E_{LUMO}^{dye} + 2E_{HOMO}^{dye}\right] - \left[E_{LUMO}^{dye} + E_{HOMO}^{dye} + E_{CBO}^{TiO_2}\right] \quad (14)$$

where $E_{CBO}^{TiO_2}$ is the conduction band edge. It is difficult to accurately determine $E_{CBO}^{TiO_2}$, because it is highly sensitive to the conditions (e.g. the pH of the solution) thus we have used $E_{CBO}^{TiO_2}$ = -4.0 eV [43] which is experimental value corresponding to conditions where the semiconductor is in contact with aqueous redox electrolytes of fixed pH 7.0 [46].

More quantitatively for a closed-shell system E_{LUMO}^{dye} corresponds to the reduction potential of the dye E_{RED}^{dye}, whereas the HOMO energy is related to the potential of first oxidation (i. e., - $E_{HOMO}^{dye} = E_{OX}^{dye}$). As a result, Eq. (14) becomes,

$$\Delta E_{RP} = \left[E_{OX}^{dye} + E_{OX}^{TiO_2}\right] \quad (15)$$

2.2 Computational Detail. Electronic structure calculations for the studied dyes were performed with the density functional theory (DFT) for the ground state, and with its TD extension (TD-DFT) for the excited state, adopting both the B3LYP [57] and CAM-B3LYP [48] combination with the 6-31G basis set. Density functional theory (DFT) calculations were performed with the Gaussian 09[49] program package. TD-DFT [50,51] computations were completed on the enhanced ground-state atomic structures to decide their pinnacle ingestion wavelengths and molar termination coefficients, with the B3LYP and CAM-B3LYP functional and 6-31 basis set. In addition, the transition properties of the dyes in solvent were computed utilizing the TD-DFT method in view of the advancement of the ground state structures in acetonitrile solvent. In all calculations, frequency checks were performed after each geometry optimization to ensure that minima on the potential energy surfaces were found. The models of electron density of various energy levels of the HOMO – LUMO were were visualized using Gauss View Version5.0 [52].

3. Results and Discussion

3.1 Geometrical Structures. All the molecular geometries have been computed with the B3LYP and CAM-B3LYP functional and 6-31G basis set as are shown in Figure 1. The level of degree conjugation is an essential factor influencing the UV absorption spectra of the dyes. The coplanarity indicated that the introduction of auxiliary heterocycle acceptor can be favourable for the electron transition, so we computed the basic dihedral edges. The advanced geometrical parameters (Scheme 2) of all the investigated dyes are gathered in Table 1. For every one of the dyes, the dihedral point's Φ1 and Φ2 framed between the acceptor group and donor group respectively in gas and solvent. The outcomes demonstrate that the donor and acceptor moieties are completely conjugated through the π bridge. This may prompt better conjugation so the assimilation wavelength will have a red shift. The coplanarity showed that the introduction of auxiliary heterocycle acceptor can be positive for the electron change.

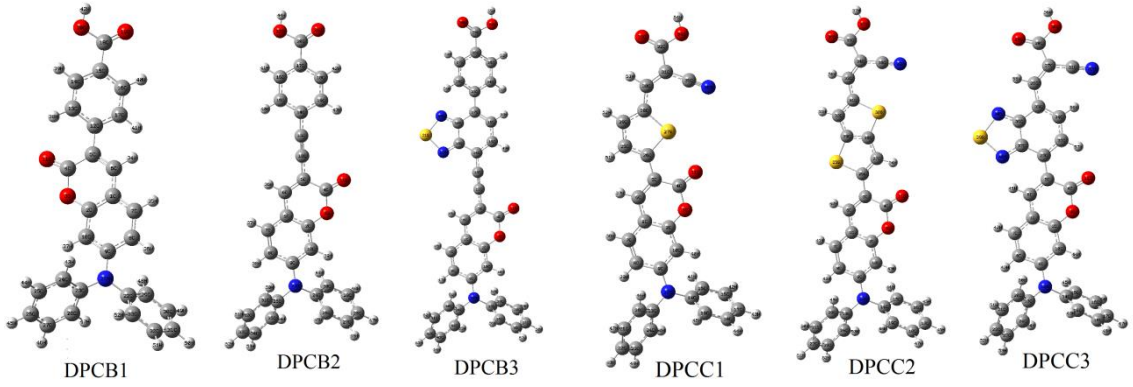

Figure 1. The optimized geometry structure of studied dyes with DFT/B3LYP functional with 6-311G basis set in gas phase.

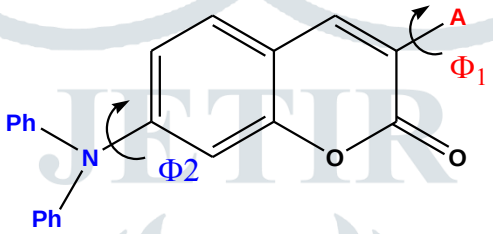

Scheme 2. Brief structure of D-π-A dyes.(Φ_1 and Φ_2 represent the dihyhedral angles)

Table 1. Calculated Dihedral Angles between the donating groups and acceptor group between coumarine unit.

dye	B3LYP/6-31G				CAM-B3LYP/6-31G			
	gas		solvent		gas		solvent	
	Φ_1	Φ_2	Φ_1	Φ_2	Φ_1	Φ_2	Φ_1	Φ_2
DPCB1	32.01	-26.23	35.27	-23.07	-146.07	-25.45	-144.37	-22.42
DPCB2	-0.36	-25.85	-40.23	-22.22	-1.94	-24.87	-171.87	-20.98
DPCB3	-28.14	-24.02	-166.72	-23.97	3.23	-27.07	0.13	
DPCC1	-179.88	-25.01	-178.04	-21.39	-9.86	-23.68	179.80	-25.01
DPCC2	-179.88	-24.61	-179.13	-21.45	-179.80	-23.55	0.44	-20.08
DPCC3	179.23	-24.72	-159.76	-21.58	-179.23	-23.63	-157.32	-20.26

3.2 Frontier molecular orbitals. Since charge separated states is one of the main factors affecting solar cell efficiency, qualitative predictions of the efficiency of sensitizers could be made using HOMO, LUMO, and HOMO-LUMO energy gaps. HOMOs must be localized on the donor and LUMOs on the acceptor to create an efficient charge separated states [53]. To clarify the donor-pi-acceptor (D-π-A) nature of the present dyes, the HOMOs and LUMOs were calculated, and the frontier orbital isosurface plots are presented in Fig.2.

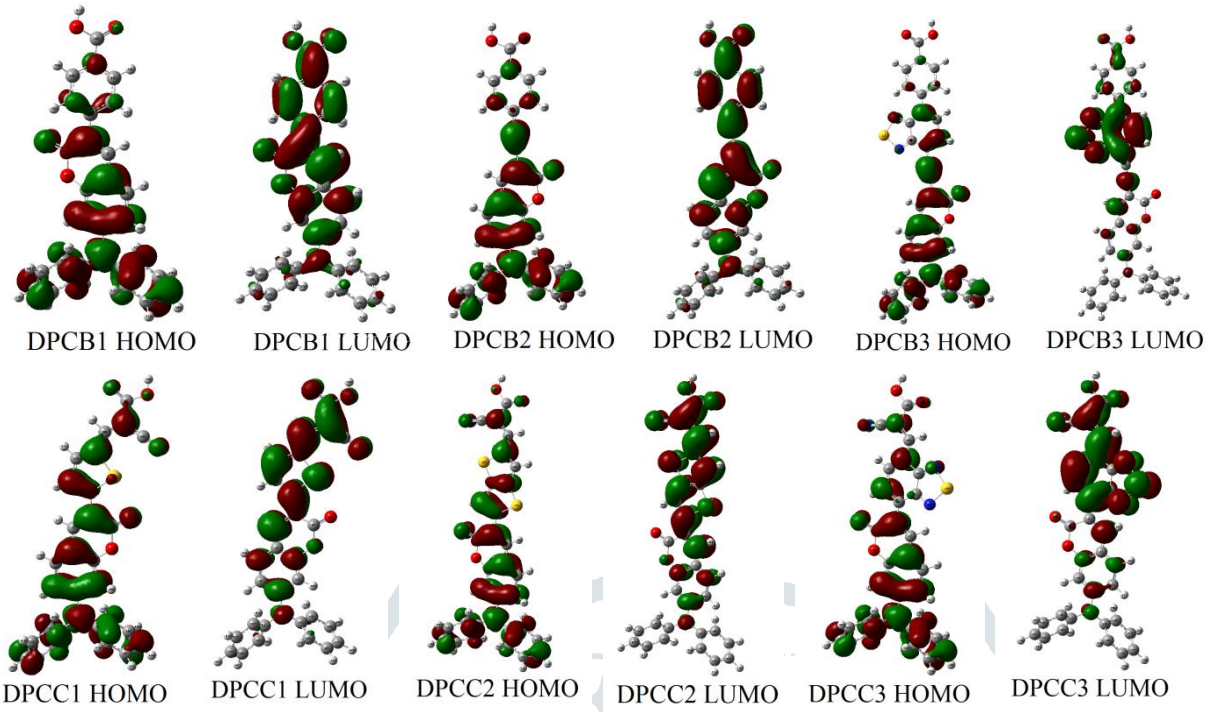

Figure 2. Frontier molecular orbitals of all studied dyes at level of TD-DFT/6-31G in solvent.

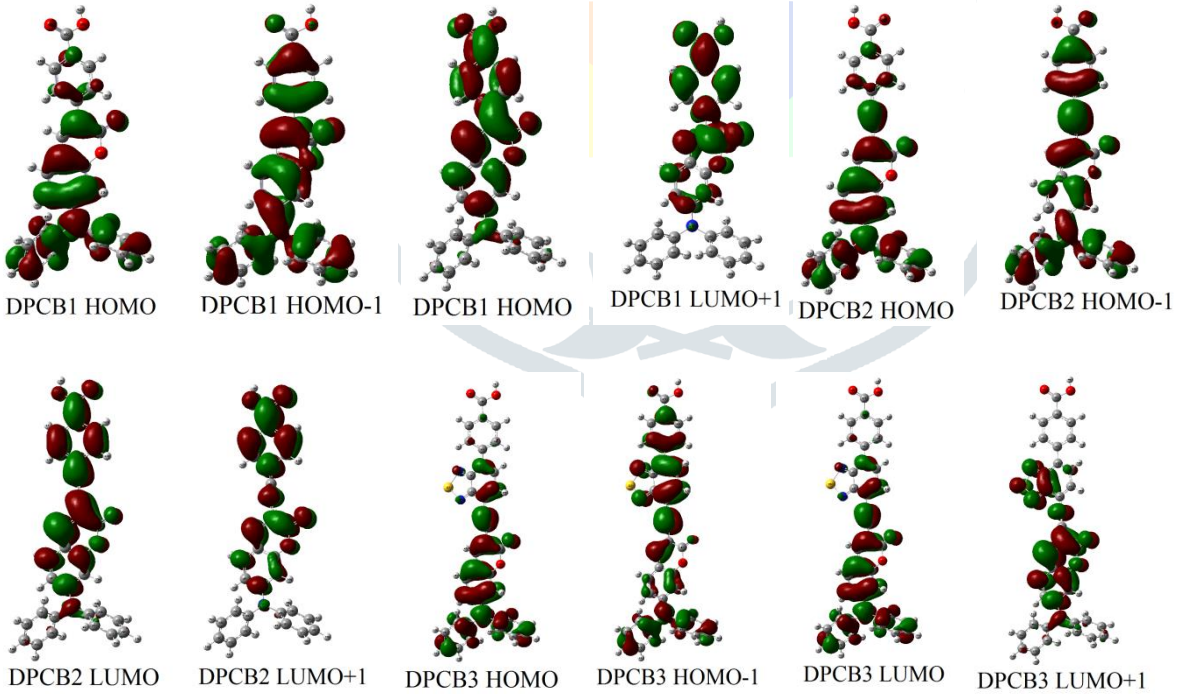

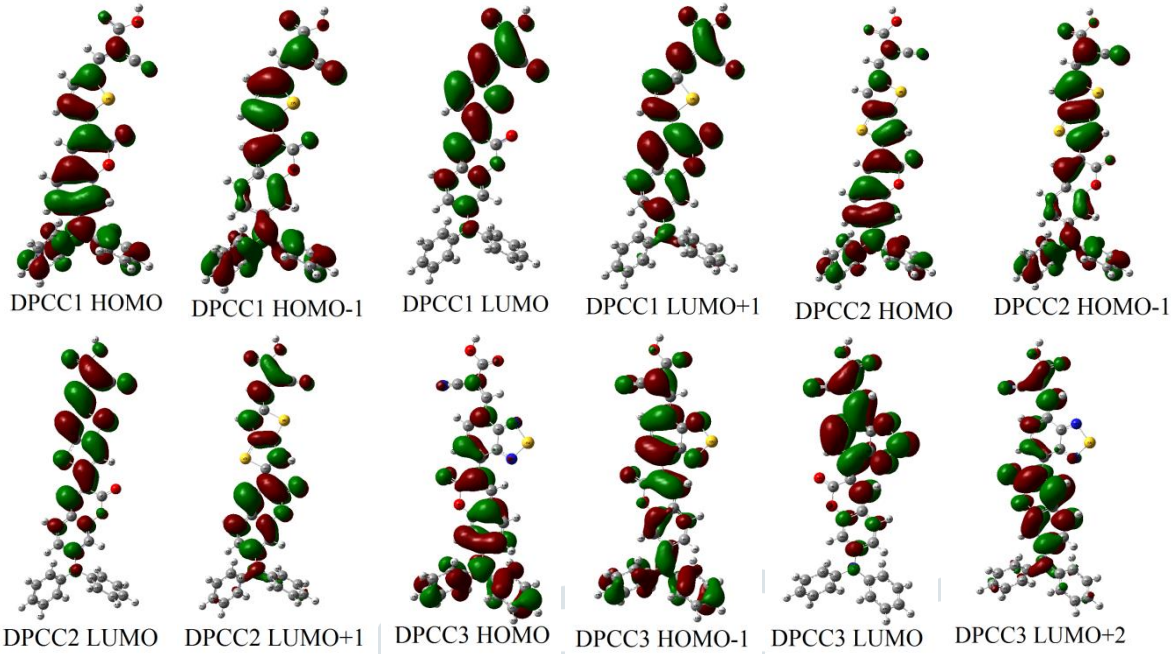

Figure 3. Frontier molecular orbitals of all studied dyes at level of TD-CAM/DFT/6-31G in solvent.

Table 2. The HOMO-LUMO energies, energy gap and dipole moment of studied dyes.

molecule	**B3LYP/6-31G**							
	Gas				solvent			
	HOMO	**LUMO**	**Egap**	**μ**	**HOMO**	**LUMO**	**Egap**	**μ**
DPCB1	-5.43968	-2.23438	3.2053	7.5505	-5.41546	-2.30567	3.1098	10.4142
DPCB2	-5.39233	-2.37996	3.0124	9.4335	-5.40893	-2.49153	2.9174	13.3522
DPCB3	-5.36838	-3.07060	2.2978	8.1507	-5.38362	-3.16448	2.2191	10.8177
DPCC1	-5.51560	-2.90624	2.6094	7.4707	-5.47669	-3.03985	2.4368	19.4741
DPCC2	-5.50308	-3.02625	2.4768	7.3061	-5.42254	-3.11986	2.3027	19.1140
DPCC3	-5.59778	-3.48150	2.1163	11.4214	-5.50553	-3.52395	1.9816	15.8877
CAM-B3LYP/6-31G								
molecule	**HOMO**	**LUMO**	**E gap**	**μ**	**HOMO**	**LUMO**	**E gap**	**μ**
DPCB1	-6.64299	-1.03651	5.6065	7.0064	-6.62422	-1.10535	5.5189	9.8003
DPCB2	-6.58585	-1.21883	5.3670	8.9005	-6.60626	-1.33039	5.2759	11.8948
DPCB3	-6.54993	-1.95899	4.5909	7.0358	-6.57578	-2.03138	4.5444	8.9162
DPCC1	-6.67919	-1.79708	4.8821	11.8140	-6.60462	-2.04471	4.5599	17.1139
DPCC2	-5.76051	-1.94620	3.8143	7.1895	-6.57932	-2.03056	4.5488	17.5572
DPCC3	-6.72980	-2.43085	4.2990	9.7961	-6.63156	-2.57698	4.0546	13.1644

From the frontier molecular orbitals illustrated, we could see that in all dyes HOMO and HOMO-1 are localized on the diphenylamine donor groups, LUMOs on the carboxylic acid and cyanoacrylic acid acceptor groups, and the coumarin chromophors constitute the π-bridges. The present structures are therefore (D-π-A) type donors with electron-rich (donor) and electron-poor (acceptor) sections connected through a conjugated (π) bridge. The HOMo and LUMO electron densities of the six dyes are shown in Fig.2. & 3 in solvent at B3LYP and CAM/B3LYP level of theory with 6-311Gbasis set.

The increased electron density of the cyanoacrylic acid anchoring group relative to that of the carboxylic acid anchoring group may be attributed to the excess nitrogen and the extended length of π-conjugation. The larger electron density lead to efficient electron injection from the dye singlet excited state to the conduction band (CB) of the electrode owing to the strong electronic coupling between the excited adsorbed dye and the 3d- orbitals, that make up the CB of the electrode surface through the anchoring group, resulting in the difference in the cell performances between the two systems. This gives an essential sign to the upgraded cell execution of the dyes containing cyanoacrylic acid anchoring groups with respect to those containing carboxylic acid anchoring groups.

3.3 Energy gaps. The photovoltaic performance of a dye sensitized solar cell is closely associated with the energy gap of HOMO and LUMO of the dye. Frontier orbital energy levels and energy gaps of the studied dyes are given in Table 2. From the results, replacing the carboxylic acid anchoring group by cyanocarboxylic acid anchoring group lead to narrowing the band gap of the highest record efficient dye DPCC3 in both gas and solvent at both level of theory, expect in CAM/B3LYP in gas; DPCC2 dye is efficient sensitizer. This nominates DPCB2, DPCB2, and DPCB2 dyes to be better candidates for DSSCs. The expected order of performance from energy gap between HOMO-LUMO is DPCC3 < DPCC2 < DPCC1 < DPCB3 < DPCB2 < DPCB1.

From the Table 2, while the addition of cyanocacrylic acid anchoring group to coumarin marginally decreases the corresponding band gap. The decrease in HOMO-LUMO energy gap mainly comes from destabilizing the HOMO. At the point when the DPCC3 dye is compared other dyes to observe that they have similar anchoring groups but attached to different thiophene moieties.

3.4. Absorption Spectra. The absorption spectra calculated for the studied in acetonitrile solvent at the TD-DFT method using PCM solvent model are shown in Figure 4. The main electron transitions, oscillator strengths (f) and absorption bands are summarized in Table 3. From the table 3 all the dyes basically have the same contribution of electronic transition from HOMO to LUMO, which means that the introduction of heteroatom in additional acceptor can greatly influence the contribution of electronic transition. The UV absorption spectra of studied dyes have significantly changed due to their higher conjugation and narrower band gaps. In particular, the λ_{max} of DPCC3 at CAM/B3LYP method, the most red-shifted absorption band

due to the auxiliary group contain two nitrogen atoms and one sulphur atom, which agree well with them possessing the narrowest HOMO-LUMO gaps. The dye DPCC3 with the intense absorption peak at 614.50 nm, also have a great red-shift compared to other studied dyes. Although the absorption spectra of other dyes are not extremely red-shift, they have lower oscillator strength.

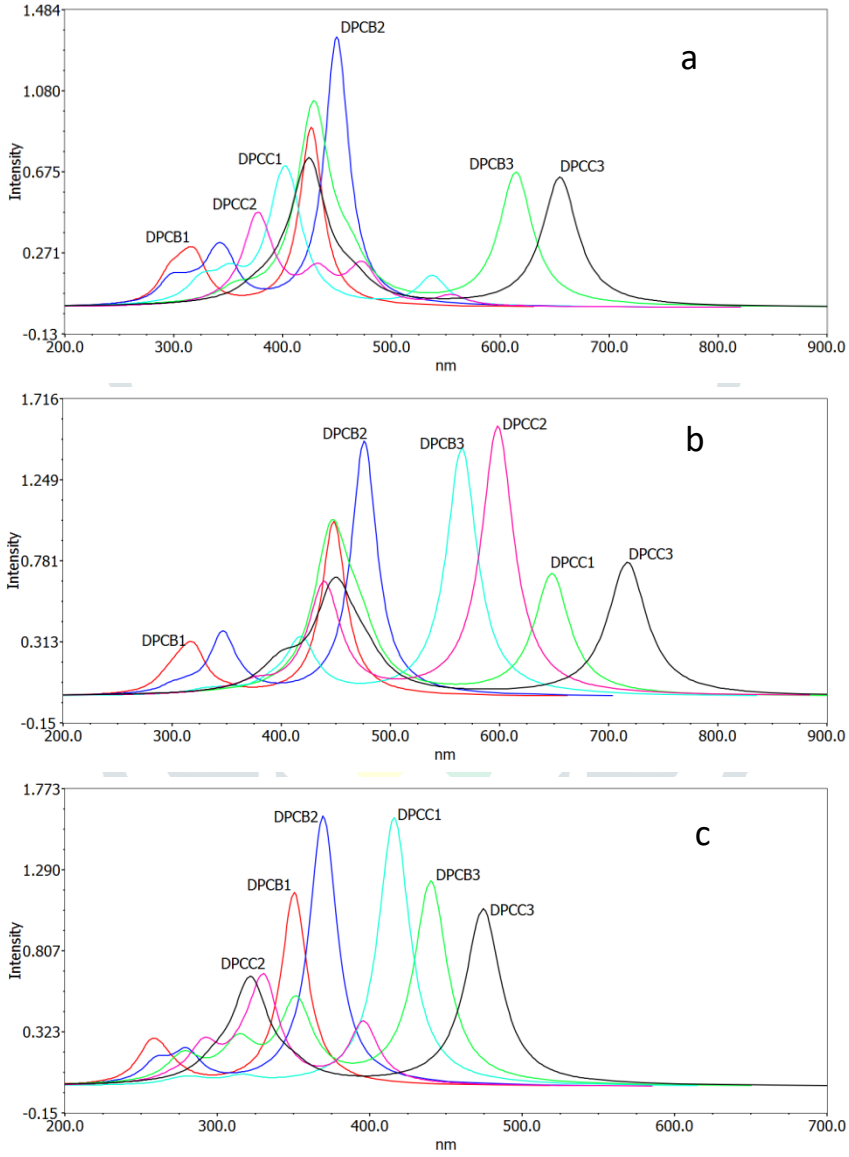

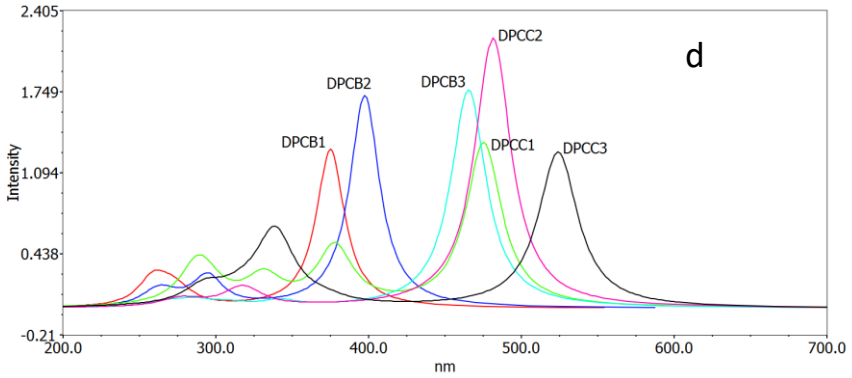

Figure 4. Absorption Spectra of all the Investigated Dyes.(a) in gas at DFT/6-311G;(b) in Acetonitrile DFT/6-311G (c) in gas at CAM-B3LYP/6-31G (d) in Acetonitrile CAM-B3LYP/6-31G.

Table 3. Main Electron Transitions, Oscillator Strengths (f) and absorption bands for the coumarin based dyes in gas and solvent.

	B3LYP							
	Gas				**Solvent**			
	nm	Oscillator Strength (f)	MO /character	% contri-bution	nm	Oscillator Strength (f)	MO /character	% contri bution
DPCB1	426.59	0.8947	HOMO→LUMO	98.78	448.33	1.0074	HOMO→LUMO	98.99
DPCB2	450.00	1.3434	HOMO→LUMO	98.74	476.21	1.4691	HOMO→LUMO	
DPCB3	614.50	0.6643	HOMO→LUMO	98.49				98.95
DPCC1	406.06	0.4428	HOMO-1→LUMO	32.90	565.64	1.4305	HOMO→LUMO	
			HOMO→LUMO+1	64.81				99.66
DPCC2	377.67	0.4243	HOMO-2→LUMO	93.31	598.55	1.5524	HOMO→LUMO	
			HOMO→LUMO	3.23				99.568
DPCC3	424.37	0.6998	HOMO-1→LUMO	2.78	717.30	0.7689	HOMO→LUMO	
			HOMO→LUMO	91.98				99.55
CAM								
	Gas					**Solvent**		
	nm	Oscillator Strength (f)	MO /character	% contri bution	nm	Oscillator Strength (f)	MO /character	% contri bution
DPCB1	350.66	1.1505	HOMO -1→LUMO	4.36	375.23	1.2834	HOMO-1 →LUMO	4.72
			HOMO →LUMO	87.71			HOMO→LUMO	87.12
			HOMO -1→LUMO	2.84			HOMO→LUMO+1	3.69
DPCB2	369.58	1.6087	HOMO -1→LUMO	3.68	397.65	1.7162	HOMO-1→LUMO	4.92
			HOMO→LUMO	86.97			HOMO→LUMO	84.62
			HOMO→LUMO+1	3.76			HOMO→LUMO+1	5.38
DPCB3	440.16	1.2132	HOMO -1→LUMO	25.70	475.56	1.3272	HOMO→LUMO	0.37
			HOMO→LUMO	66.91			HOMO→LUMO+1	0.56
			HOMO→LUMO+1	2.60			HOMO→LUMO+2	0.13
DPCC1	416.18	1.5999	HOMO→LUMO	7.09	465.58	1.7674	HOMO -1→LUMO	10.72
			HOMO→LUMO	84.60			HOMO→LUMO	80.90
			HOMO→LUMO+1	3.20			HOMO→LUMO+1	3.91
DPCC2	330.62	0.6059	HOMO-5→LUMO	5.81	481.56	2.1853	HOMO-1→LUMO	11.33
			HOMO-3→LUMO	37.88			HOMO→LUMO	78.59
			HOMO→LUMO	19.89			HOMO→LUMO+1	5.09
			HOMO→LUMO+1	25.31				
DPCC3	474.60	1.0520	HOMO-1→LUMO	17.52	524.15	1.2609	HOMO-1→LUMO	18.10
			HOMO→LUMO	78.13			HOMO→LUMO	80.90
							HOMO→LUMO+2	1.00

3.5. Charge injection (ΔG_{inject}) . To searches out the connection between the anchoring groups and the electron injection efficiency, dye regeneration, we calculated the $\triangle G_{inject}$ and $\triangle G_{reg}$ of the dyes and the data

were listed in Table 4. The values of E^{dye*} are all more negative than TiO_2 conduction band, showing that they are support to electron injection. From Table 4, the free energy change $\triangle G_{inject}$ of all the dyes are in the range of -0.64992eV to -1.77982eV. All the $\triangle G_{inject}$ values are very negative (< -1 eV). This means that an efficient electron injection takes place from the sensitizers into the TiO_2. The driving force of DPCC2 is the most negative, suggesting that it will lead to faster electron injection among all the dyes.

3.6. Dye regeneration (ΔG^{regen}). The efficiency of dye regeneration or the free energy change of dye regeneration ΔG^{regen} can affect the rate constant of redox process between the oxidized dyes and electrolyte. Taking into account the ideal redox potential (3.5 eV vs vacuum), ΔG^{regen} can be calculated from the relation

$$\Delta G^{regen} = E_{ox}^{dye} - E_{redox}^{electrolyte} \quad (16)$$

Where $E_{redox}^{electrolyte}$ is the redox potential of the electrolyte. The values of the present dyes are listed in Table 4. As shown, replacing cyanoacrylic group generates a considerable change of ΔG^{regen}. This in turn implies that the corresponding excitations generate charge separated states, and contribute to the sensitization of photo-to current conversion processes. In other words, cyanoacrylic anchoring group replacements shift the absorption bands to longer wavelengths, and make the dyes DPCC3, DPCC2 and DPCC1 good potential candidates for harvesting more light in the UV-vis. region of the solar spectrum.

3.7 Light Harvesting Efficiency (LHE) and Oscillator Strength. The Jsc is influenced by the $\triangle G^{inject}$, absorption wavelength and corresponding LHE. The light harvesting efficiency (LHE) is the efficiency of dye to response the light. It is another factor which indicates the efficiency of DSSC. The light harvesting efficiency (LHE) of the dye should be as high as feasible to maximize the photo-current response.

Table 4. Calculated Electronic Properties of the coumarin based Dyes in gas and acetonitrile solvent

DFT/B3LYP/6-311G									
Gas									
Molecul	E^{dye}(eV)	E^{dye*} (eV)	ΔG^{inject} (eV)	LHE	V_{oc} (eV)	$\Delta G^{regen.}$ (eV)	ΔE_{RP}	$\lvert V_{RP} \rvert$	τ(ns)
DPCB 1	5.43968	2.53328	-1.46672	0.872562	-6.23438	0.63968	1.4397	0.7198	3.0489
DPCB 2	5.39233	2.63713	-1.36287	0.954648	-6.37996	0.59233	1.3923	0.6962	2.2595
DPCB 3	5.36838	3.35078	-0.64922	0.783379	-7.0706	0.56838	1.3684	0.6842	8.5211
DPCC 1	5.51560	2.4623	-1.53770	0.639255	-6.90624	0.71560	1.5156	0.7578	5.5819
DPCC 2	5.50308	2.22018	-1.77982	0.623556	-7.02625	0.70308	1.5031	0.7515	5.0390
DPCC 3	5.59778	2.67618	-1.32382	0.800382	-7.4815	0.79778	1.5978	0.7989	3.8576

solvent									
Molecul	E^{dye}(eV)	E^{dye*} (eV)	ΔG^{inject} (eV)	LHE	V_{oc} (eV)	$\Delta G^{regen.}$ (eV)	ΔE_{RP}	$\lvert V_{RP} \rvert$	τ(ns)
DPCB 1	5.41546	2.64996	-1.35004	0.901689	-6.30567	0.61546	1.4155	0.7077	2.9907
DPCB 2	5.40893	2.80533	-1.19467	0.966045	-6.49153	0.60893	1.4089	0.7045	2.3138
DPCB 3	5.38362	2.60602	-1.39398	0.876750	-7.16448	0.58362	1.3836	0.6918	3.2850
DPCC 1	5.47669	3.28479	-0.71521	0.962889	-7.03985	0.67669	1.4767	0.7383	3.3527
DPCC 2	5.42254	3.35114	-0.64886	0.971971	-7.11986	0.62254	1.4225	0.7113	3.4594
DPCC 3	5.50553	3.77703	-0.22297	0.829745	-7.52395	0.70553	1.5055	0.7528	10.0305
CAM/B3LYP/6-311G									
Gas									
Molecul	E^{dye}(eV)	E^{dye*} (eV)	ΔG^{inject} (eV)	LHE	V_{oc} (eV)	$\Delta G^{regen.}$ (eV)	ΔE_{RP}	$\lvert V_{RP} \rvert$	τ(ns)
DPCB 1	6.64299	3.10719	-0.89281	0.929287	-5.03651	1.84299	2.6430	1.3215	1.6020
DPCB 2	6.58585	3.23105	-0.76895	0.975379	-5.21883	1.78585	2.5859	1.2929	1.2726
DPCB 3	6.54993	3.73313	-0.26687	0.938793	-5.95899	1.74993	2.5499	1.2750	2.3938
DPCC 1	6.67919	3.70009	-0.29991	0.974875	-5.79708	1.87919	2.6792	1.3396	1.6228
DPCC 2	5.76051	2.01041	-1.98959	0.752201	-5.9462	0.96051	1.7605	0.8803	2.7042
DPCC 3	6.72980	4.1174	0.1174	0.911284	-6.43085	1.92980	2.7298	1.3649	3.2095
Solvent									
Molecu	E^{dye}(eV)	E^{dye*} (eV)	ΔG^{inject} (eV)	LHE	V_{oc} (eV)	$\Delta G^{regen.}$ (eV)	ΔE_{RP}	$\lvert V_{RP} \rvert$	τ(ns)
DPCB 1	6.62422	3.32002	-0.67998	0.947929	-5.10535	1.82422	2.6242	1.3121	1.6445
DPCB 2	6.60626	3.48836	-0.51164	0.980778	-5.33039	1.80626	2.6063	1.3031	1.3811
DPCB 3	6.57578	3.96868	-0.03132	0.952930	-6.03138	1.77578	2.5758	1.2879	2.5543
DPCC 1	6.60462	3.94162	-0.05838	0.982916	-6.04471	1.80462	2.6046	1.3023	1.8384
DPCC 2	6.57932	4.00462	0.00462	0.993473	-6.03056	1.77932	2.5793	1.2897	1.5906
DPCC 3	6.63156	4.26616	0.26616	0.945160	-6.57698	1.83156	2.6316	1.3158	3.2662

3.8. Excited State Lifetimes (τ). The lifetime (τ) of the excited state(s) is one of the vital factors for considering the efficiency of charge transfer [54].In order to realize long-term stability; the dyes should remain stable in the cationic form for a long time. A dye with a longer lifetime in the excited state is expected to be more facile for charge transfer. The excited state lifetimes of the dyes can be can be assessed utilizing the equation ($\tau=1.499/f\,E^2$), where E is the excitation energy of the different electronic states (cm^{-1}) and f is oscillator strength of the electronic state. The results of the lifetime (τ) all the investigated dyes are presented in Table 4. Clearly the electron lifetime for the DPCC3 is high compare to other dyes. Because of DPCC3 dye retards the charge recombination process and enhances the efficiency of the DSSCs.

4. Conclusion

In the present research paper, we have been designed a series courmarin based dyes with improved photophysical properties by introducing thiophene heterocyclic acceptors with different nature of anchoring groups which presents an alternative way to shift the photo-response of the dye-sensitizers to the NIR. All the designed dyes shows very narrow HOMO-LUMO energy gap, leading to a broad absorption band in the

range of 400-620 nm. We found that ΔG^{inject} values are negative for all the designed dyes. This is an important result because a negative value of this parameter is an indication of spontaneous electron injection from the dye to TiO_2.The light harvesting efficiency (LHE) is the efficiency of dye to response the light. The light harvesting efficiency (LHE) of the dye should be as high as feasible to maximize the photo-current response. We have noted that all the dyes LHE values are near to one. This calculation procedure can be used as a model system for understanding the relationships between electronic properties and molecular structure and also can be employed to explore their suitability in electroluminescent devices and in related applications. Finally, the procedures of theoretical calculations can be employed to predict the electronic properties on the other compounds, and further to design novel materials for sensitizers for solar cells.

References

1. Gratzel M. Photoelectrochemical cells. 2001. Photoelectrochemical cells Nature, 414, 338-344.
2. Ahn KS, Yoo SJ, Kang MS, Lee JW and Sung YE. 2007.Tandem dye-sensitized solar cell-powered electrochromic devices for the photovoltaic-powered smart window. J. Power Sources. 168, 533–536.
3. Baetens R, Jelle BP and Gustavsen, A. 2010. Properties, requirements and possibilities of smart windows for dynamic daylight and solar energy control in buildings: A state-of-the-art review. Sol. Energy Mater. Sol. Cells. 94, 87–105.
4. O'Regan B and Gratzel M. 1991.A low-cost, high-efficiency solar cell based on dye-sensitized colloidal TiO_2 films. Nature. 353, 737–740.
5. Adachi M, Murata Y, Takao J, Jiu J, Sakamoto M and Wang F. 2004. Highly Efficient Dye-Sensitized Solar Cells with a Titania Thin-Film Electrode Composed of a Network Structure of Single-Crystal-like TiO_2Nanowires Made by the "Oriented Attachment" Mechanism.J. Am. Chem. Soc. 126(45), 14943-14949.
6. Law M, Greene LE, Johnson JC, Saykally R and Yang P. 2005.Nanowire dye-sensitized solar cells. Nat. Mater. 4(6), 455-459.
7. Zhang DS, Downing JA, Knur, FJ, and McHale, JL. 2006.Room-Temperature Preparation of Nanocrystalline TiO_2 Films and the Influence of Surface Properties on Dye-Sensitized Solar Energy Conversion.J. Phys. Chem. B,110, 21890-21898.
8. Xue J Uchida S, Rand BP and Forrest SR. 2004. 4.2% efficient organic photovoltaic cells with low series resistances Appl. Phys. Lett, 84, 3013-3015.
9. Xue J, Uchida S, Rand BP and Forrest SR. 2004.Asymmetric tandem organic photovoltaic cells with hybrid planar-mixed molecular heterojunctions .Appl. Phys. Lett, 85, 5757-5759.
10. Reyes-Reyes M, Kim K and Carroll DL. 2005.High-efficiency photovoltaic devices based on annealed poly(3-hexylthiophene) and 1-(3-methoxycarbonyl)-propyl-1- phenyl-(6,6)C61(6,6)C61blends.Appl. Phys. Lett, 87, 083506-083509.
11. Hoertz PG and Mallouk TE. 2005. Light-to-Chemical Energy Conversion in Lamellar Solids and Thin Films. Inorg. Chem ,44, 6828-6840.
12. O'Regan BC, Bakker K, Kroeze J, Smit H, Sommeling P and Durrant JR. 2006. Measuring Charge Transport from Transient Photovoltage Rise Times. A New Tool To Investigate Electron Transport in Nanoparticle Films .J. Phys. Chem. B,1109 (34), 17155-17160.

13. Hagfeldt A and Gra¨tzel M. 1995.Light-Induced Redox Reactions in Nanocrystalline Systems Chem. ReV, 95, 49-68.
14. Kalyanasundaram K and Gra¨tzel M. 1998.Applications of functionalized transition metal complexes in photonic and optoelectronic devices Coord. Chem. ReV, 77, 347-414.
15. Hagfeldt A and Gra¨tzel M. 2000. Molecular Photovoltaics.Acc. Chem. Res, 33(5), 269-277.
16. Gra¨tzel M. 2003. Dye-sensitized solar cells. J. Photochem. Photobiol. C , 4, 145-153.
17. Nazeeruddin MK, Kay A, Rodicio I, Humphry Baker R, Mu¨ller E, Liska P, Vlachopoulos N and Gra¨tzel M. 1993.Conversion of light to electricity by cis-X2bis(2,2'-bipyridyl-4,4'-dicarboxylate)ruthenium(II) charge-transfer sensitizers (X = Cl^-, Br^-, I^-, CN^-, and SCN^-) on nanocrystalline titanium dioxide electrodes.J. Am. Chem. Soc, 1159 (14), 6382-6390.
18. Barbe´ CJ, Arendse F, Comte P, Jirousek M, Lenzmann F, Shklover V and Gra¨tzel M. 1997. Nanocrystalline Titanium Oxide Electrodes for Photovoltaic Applications.J. Am. Ceram. Soc, 80, 3157-3171.
19. Nazeeruddin MK, Pe´chy P, Renouard T, Zakeeruddin SM, Humphry Baker R, Comte P, Liska P, Cevey L, Costa E, Shklover V, Spiccia L, Deacon GB, Bignozzi CA and Gra¨tzel M. 2001.Engineering of Efficient Panchromatic Sensitizers for Nanocrystalline TiO_2 based Solar Cells. J. Am. Chem. Soc, 1239(8), 1613-1624.
20. Klein C. Nazeeruddin Md. K, Di Censo D, Liska P and Gra¨tzel M. 2004. Amphiphilic Ruthenium Sensitizers and Their Applications in Dye-Sensitized Solar Cells.Inorg. Chem, 43(14), 4216-4226.
21. Mathew S, Aswani Y, Peng G, Robin HB, basile FE, Negar AA, Ivano T,Ussula R, Md. and Khaja N. 2014. Dye-sensitized solar cells with 13% efficiency achieved through the molecular engineering of porphyrin sensitizers. *J. Nat. Chem*,6, 242–247 .
22. Nazeeruddin MK, Pechy P and Gratzel M. 1997.Efficient panchromatic sensitization of nanocrystallineTiO_2 films by a black dye based on atrithiocyanato–ruthenium complex.Chem.Commun,18,1705–1706.
23. Hara K, Sayama K, Ohga Y, Shinpo A, Suga S and Arakawa H. 2001. A coumarin-derivative dye sensitized nanocrystalline TiO_2 solar cell having a high solar-energy conversion efficiency up to 5.6%Chem. Commun, 6,569–570.
24. Hara K, Sato T, Katoh R, Furube A, Ohga Y, Shinpo A, Suga S, Sayama K, Sugihara H and Arakawa H. 2003.Molecular Design of Coumarin Dyes for Efficient Dye-Sensitized Solar Cells. J. Phys. Chem. B,107(2), 597–606.
25. Hara K, Kurashige M, Danoh Y, Kasada C, Shinpo A, Suga S, Sayama K and Arakawa H. 2003.Design of new coumarin dyes having thiophene moieties for highly efficient organic-dye-sensitized solar cells. New J. Chem, 27, 783–785.
26. Hara K, Wang ZS, Sato T, Furube A, Katoh R, Sugihara H, Danoh Y, Kasada C, Shinpo A and Suga S. 2005.Oligothiophene-Containing Coumarin Dyes for Efficient Dye-Sensitized Solar Cells. J. Phys. Chem. B,109, 15476–15482.
27. Martsinovich N and Troisi 2011. A. Theoretical studies of dye-sensitised solar cells: From electronic structure to elementary processes. Energy Environ. Sci, 4, 4473–4495.
28. Suresh T, Chitumalla RK, Hai NT, Jang J, Lee TJ and Kim JH. 2016.Impact of neutral and anion anchoring groups on the photovoltaic performance of triphenylamine sensitizers for dye-sensitized solar cells. RSC Adv, 6, 26559–26567.
29. Hara K, Sato T, Katoh R, Furube A, Ohga Y, Shinpo A, Suga S, Sayama K, Sugihara H and Arakawa H. 2003.Molecular design of coumarin dyes for efficient dye-sensitized solar cells. J. Phys. Chem. B, 107, 597–606.
30. Kurashige Y, Nakajima T, Kurashige S, and Hirao K. 2007. Theoretical investigation of the excited states of coumarin dyes for dye-sensitized solar cells. J. Phys. Chem. A , 111, 5544–5548.
31. Preat J, Loos PF, Assfeld X, Jacquemin D and Perpète EA. 2007.A TD-DFT investigation of UV spectra of pyranoïdic dyes: A NCM vs. PCM comparison. J. Mol. Struct. Theochem, 808, 85–91.
32. Zhang X, Zhang JJ, and Xia YY. 2008. Molecular design of coumarin dyes with high efficiency in dye- sensitized solar cells. J. Photochem. Photobiol. A Chem, 194, 167–172.

33. Sanchez-de-Armas R, San Miguel MA, Oviedo J and Sanz JF. 2012.Coumarin derivatives for dye sensitized solar cells: A TD-DFT study. Phys. Chem. Chem. Phys, 14, 225–233.
34. Narayan MR. Review: 2012.Dye Sensitized Solar Cells Based on Natural Photosensitizers. Renew. Sust. Energ. Rev, 16, 208-215.
35. Zhang J, Li HB, Sun SL, Geng Y, Wu Y and Su ZM. 2012.Density functional theory characterization and design of high-performance diarylamine-fluorene dyes with different π spacers for dye-sensitized solar cells.J. Mater. Chem, 22(2), 568-576.
36. Julien P, Denis J and Eric AO. 2010.Towards new efficient dye-sensitised solar cells Energy &Environmental Science,7, 891-904.
37. Katoh R, Furube A, Yoshihara T, Hara K, Fujihashi G, Takano S, Murata S, Arakawa H and Tachiya M. 2004.Efficiencies of Electron Injection from Excited N3 Dye into Nanocrystalline Semiconductor (ZrO_2, TiO_2, ZnO, Nb_2O_5, SnO_2, In_2O_3) Films.J. Phys. Chem. B, 108 (15), 4818-4822.
38. Barbara PF, Meyer TJ and Ratner MA. 1996. Contemporary Issues in Electron Transfer Research.J Phys Chem,100(31),13148-13168.
39. De Angelis F, Fntacci S and Selloni A. 2008.Alignment of the dye's molecular levels with the TiO(2) band edges in dye-sensitized solar cells: a DFT-TDDFT study. Nanotechnology, 19(42), 424002-424009.
40. Marinado T, Nonomura K, Nissfolk J, Karlsson MK, Hagberg DP, Sun L, Mori S and Hagfeldt A. 2010. How the Nature of Triphenylamine-Polyene Dyes in Dye-Sensitized Solar Cells Affects the Open-Circuit Voltage and Electron Lifetimes. Langmuir, 26, 2592-2598.
41. Zhang J, Li HB, Sun SL, Geng Y, Wu Y and Su ZM. 2012. Density Functional Theory Characterization and Design of High-Performance Diarylamine-Fluorene Dyes with Different [Small Pi] Spacers for Dye-Sensitized Solar Cells. J. Mater. Chem, 22, 568-576.
42. Marinado T, Nonomura K, Nissfolk J, Karlsson MK, Hagberg DP, Sun L, Mori S and Hagfeldt A. 2009.How the Nature of Triphenylamine-Polyene Dyes in Dye-Sensitized Solar Cells Affects the Open-Circuit Voltage and Electron Lifetime.Langmuir, 26 (4) , 2592-2598.
43. Pourtois G, Beljonne J, Ratner, MA, and Bredas, JL. 2002. Photoinduced Electron-Transfer Processes along Molecular Wires Based on Phenylenevinylene Oligomers: A Quantum-Chemical Insight.J Am Chem Soc, 124(16), 4436-4447.
44. Hsu CP. 2009.The Electronic Couplings in Electron Transfer and Excitation Energy Transfer Acc Chem Res, 42(4), 509-518.
45. Marcus RA.1993. Electron transfer reactions in chemistry. Theory and experiment.Rev Mod Phys, 65, 599-610.
46. Asbury JB, Wang YQ, Hao E, Ghosh H and Lian T. 2001. Evidences of hot excited state electron injection from sensitizer molecules to TiO_2 nanocrystalline thin films.Res Chem Intermed, 27(4-5), 393-406.
47. Lee C, Yang W and Parr RG. 1988.Development of the colle-salvetti correlation-energy formula into a functional of the electron density. Phys. Rev, B37, 785–789.
48. Yanai T, Tew DP and Handy NC. 2004. A New Hybrid ExchangeCorrelation Functional Using the Coulomb-attenuating Method (CAM-B3LYP). Chem. Phys. Lett, 393, 51−57.
49. Frisch MJ, Trucks GW and Schlegel HB. et al.,2010. "Gaussian 09," Revision C.01,Gaussian,Wallingford,Conn,USA.
50. Casida ME, Jamorski C, Casida KC and Salahub DR. 1998. Molecular excitation energies to high-lying bound states from time-dependent Density-Functional Response theory: Characterization and correlation of the time dependent local density approximation ionization threshold. J. Chem. Phys, 108, 4439–4449.
51. Chipman DM. 2000.Reaction Field Treatment of Charge Penetration. J. Chem. Phys, 112, 5558−5565.
52. Dennington R, Keith T, Millam J. "GaussView,"Version5,2009. Semi chem, Shawnee Mission, Kan, USA.

53. Tachinaba Y, Haque SA, Mercer IP, Durrant JR and Klug DR. 2000. Electron Injection and Recombination in Dye Sensitized Nano crystalline Titanium Dioxide Films: A Comparison of Ruthenium Bipyridyl and Porphyrin Sensitizer Dyes, J. Phys. Chem.B ,104,1198-1205.
54. Shalabi AS, El Mahdy AM, Taha HO and Soliman KA.,2015. The Effects of Macrocycle and Anchoring Group Replacements on the Performance of Porphyrin Based Sensitizer: Dft and TD-DFT Study. J. Phys. Chem. Solids, 76, 22-33.